

# Hybrid Ceramic Polymers: New, Nonbiofouling, and Optically Transparent Materials for Microfluidics

Tiina Sikanen,<sup>\*,†</sup> Susanna Aura,<sup>‡</sup> Liisa Heikkilä,<sup>†,§</sup> Tapio Kotiaho,<sup>†,§</sup> Sami Franssila,<sup>||</sup> and Risto Kostiainen<sup>†</sup>

Division of Pharmaceutical Chemistry, Faculty of Pharmacy, University of Helsinki, P.O. Box 56, FI-00014, Finland, Department of Micro and Nanosciences, School of Science and Technology, Aalto University, P.O. Box 13500, FI-00076, Finland, Laboratory of Analytical Chemistry, Department of Chemistry, University of Helsinki, P.O. Box 55, FI-00014, Finland, and Department of Materials Science and Engineering, School of Science and Technology, Aalto University, P.O. Box 16200, FI-00076, Finland

A new, commercial hybrid ceramic polymer, Ormocomp, was introduced to the fabrication of microfluidic separation chips using two independent techniques, UV lithography and UV embossing. Both fabrication methods provided Ormocomp chips with stable cathodic electroosmotic flow which enabled examination of the Ormocomp biocompatibility by means of microchip capillary electrophoresis (MCE) and (intrinsic) fluorescence detection. The hydrophobic/hydrophilic properties of Ormocomp were examined by screening its interactions with bovine serum albumin and selected amino acids of varying hydrophobicity. The results show that the ceramic, organic–inorganic polymer structure natively resists biofouling on microchannel walls even so that the Ormocomp microchips can be used in intact protein analysis without prior surface modification. With theoretical separation plates approaching  $10^4 \text{ m}^{-1}$  for intact proteins and  $10^6 \text{ m}^{-1}$  for amino acids and peptides, our results suggest that Ormocomp microchips hold record-breaking performance as microfluidic separation platforms. In addition, Ormocomp was shown to be suitable for optical fluorescence detection even at near-UV range (ex 355 nm) with detection limits at a nanomolar level ( $\sim 200 \text{ nM}$ ) for selected inherently fluorescent pharmaceuticals.

Microfluidic devices are extensively applied to bioanalytical applications in order to improve existing technology through increased speed of analysis (higher throughput) and aggressive integration of several unit operations on a single microchip (e.g., sample preconcentration, derivatization, separation, detection). The development of bioseparation methods, many of which rely on electrophoretic techniques, is of high importance in order to explore the properties of amino acids, peptides, and proteins which are the key elements in all living organisms. Since implementation of electrophoretic separation techniques on microfluidic devices is relatively straightforward, microchip capillary electrophoresis

(MCE), in combination with optical (fluorescence) detection, has particularly found its place in bioanalysis.<sup>1,2</sup>

The first microchip-based capillary electrophoresis (CE) separations<sup>3,4</sup> were realized using glass or fused silica (FS) devices which emulated the hydrophilic and relatively inert environment of silica capillaries. Processing of glass or FS is, however, somewhat laborious and does not exactly lend itself to rapid and cost-effective mass production. During the past decade, there has been a keen interest on finding more economic alternatives to glass or FS as chip fabrication materials. This has led to extensive research on less expensive polymer-based materials and the progressive development of polymer microfabrication techniques.<sup>5,6</sup>

Today, there is a substantial number of different polymers that have been utilized for the fabrication of microfluidic devices, plenty of them presently in regular use and commercially available. There are, however, certain requirements that govern the material choice from the analytical point of view, namely, the materials properties as well as the ease of mass production. The latter is an analytical issue because it affects not only the cost but also the reproducibility of chip-based analyses. The materials properties, herein, mainly include chemical stability, surface chemistry, and optical properties. As most analytical operations are performed close to room temperature, the differences in glass transition temperatures or thermal expansion coefficients between materials can be considered less relevant from the analytical point of view. Most polymers also exhibit rather similar properties with respect to thermal (approximately  $0.1\text{--}0.2 \text{ WK}^{-1}\text{m}^{-1}$ ) and electrical conductivity (resistivity on the order of  $10^{12}\text{--}10^{18} \Omega \text{ cm}^{-1}$ ). Consequently, chemical stability and surface chemistry are probably the most important materials properties as they greatly define the applications in which the particular material can, or cannot, be used.

In most cases, it is the high hydrophobicity of microfluidic chips that complicate their use in bioanalyses, especially that of

\* Corresponding author. E-mail: tiina.sikanen@helsinki.fi. Tel: 358-9-191 59169. Fax: 358-9-191 59556.

<sup>†</sup> Division of Pharmaceutical Chemistry, University of Helsinki.

<sup>‡</sup> Department of Micro and Nanosciences, Aalto University.

<sup>§</sup> Department of Chemistry, University of Helsinki.

<sup>||</sup> Department of Materials Science and Engineering, Aalto University.

- (1) Pumera, M. *Electrophoresis* **2007**, *28*, 2113–2124.
- (2) Huikko, K.; Kostiainen, R.; Kotiaho, T. *Eur. J. Pharm. Sci.* **2003**, *20*, 149–171.
- (3) Harrison, D. J.; Manz, A.; Fan, Z. H.; Ludi, H.; Widmer, H. M. *Anal. Chem.* **1992**, *64*, 1926–1932.
- (4) Manz, A.; Harrison, D. J.; Verpoorte, E. M. J.; Fetting, J. C.; Paulus, A.; Ludi, H.; Widmer, H. M. *J. Chromatogr.* **1992**, *593*, 253–258.
- (5) Shadpour, H.; Musyimi, H.; Chen, J. F.; Soper, S. A. *J. Chromatogr., A* **2006**, *1111*, 238–251.
- (6) Becker, H.; Gartner, C. *Anal. Bioanal. Chem.* **2008**, *390*, 89–111.

intact proteins. This is because high hydrophobicity often means undesired nonspecific adsorption of the proteins onto the microchannel surface when their hydrophobic moieties (i.e., amino acid residues on the protein structure) interact with the hydrophobic surface functionalities resulting in loss of the active protein conformation (protein fouling). Efforts have been made to overcome such problems by various physical (prominently oxygen plasma treatment) or chemical (prominently coating by polyacrylamide) surface modifications, but their effect is often temporary or they require a lot of manual postprocessing, respectively.<sup>7,8</sup> Often, changes in hydrophobicity also have implications on the surface charge (zeta potential) and vice versa. Greater hydrophilicity typically means more positive or negative charges on the surface (greater zeta potential) and, thus, greater electroosmotic flow (EOF),<sup>9,10</sup> though coatings resulting in nonionic surfaces also exist.<sup>11,12</sup> Nevertheless, any postprocessing treatment required to tailor the surface chemistry toward better biocompatibility increases manual work load and affects the analytical reproducibility. There is still a great demand on new, more economic polymer materials that hold inert and stable surface chemistry with inherent resistance to biofouling and that are, therefore, truly applicable to mass production.

In this study, the physicochemical properties of a new, commercial hybrid material, Ormocomp (from Microresist Technology GmbH), were examined with a view to microfluidic bioanalytical applications. Ormocomp belongs to the family of organically modified ceramics (ORMOCERs<sup>13,14</sup>), the properties of which can be tailored to different applications, such as optical devices<sup>15</sup> or antistatic and antiadhesive coatings.<sup>16</sup> ORMOCERs were first developed by Fraunhofer Institute in 1980s.<sup>17</sup> The manufacturing process includes sol-gel preparation of the inorganic backbone (typically Si-O-Si) followed by cross-linking of the organic side chains. By varying the amount of inorganic and organic elements, the properties of ORMOCERs can be adjusted in a wide range. The original idea was to combine the properties of organic polymers (functionalization, ease of processing at low temperatures, toughness) with those of glass-like materials (hardness, chemical and thermal stability, transparency).<sup>14</sup> Following commercialization by Microresist Technology GmbH, selected ORMOCERs have become available for common use, but so far, the number of papers making use of ORMOCER-based microfluidics has been limited. Apart from some micro- and nanostructured ORMOCER surfaces

exploited to tissue engineering<sup>18,19</sup> or laser desorption ionization-mass spectrometry,<sup>20,21</sup> ORMOCERs have not been used in microfluidic applications. In our previous study, we used the commercial Ormocomp in order to implement lidless microfluidic structures on silicon or glass substrates.<sup>22</sup> MCE separation of fluorescein isothiocyanate (FITC)-labeled peptides and pH-dependent EOF were also tentatively shown using the lidless, lithographically defined Ormocomp microchannels (floor and walls) with the roof made from poly(dimethyl siloxane) (PDMS). However, prominent adsorption of the peptides on PDMS roof was observed when such mixed material channels were used. Here, for the first time, the commercially available Ormocomp was used for fabrication of fully enclosed microfluidic channels by UV-lithography or UV-embossing techniques. An adhesive Ormocomp-Ormocomp bonding method was utilized to implement microfluidic channels made merely from Ormocomp. With a view to bioanalytical applications, the physicochemical properties of Ormocomp chips, fabricated by either of the patterning methods, were examined by means of standard microchip electrophoresis and fluorescence detection at visible (ex 488 nm) or near-UV (ex 355 nm) range. Most importantly, the high optical transmission of Ormocomp is a valued property in microfluidic applications. Namely, apart from PDMS and some cycloolefin (co)polymers (COP, COC), most polymer materials exhibit strong absorbance at UV and near-UV wavelengths<sup>5,23</sup> which limits their use in combination with optical detection techniques. Direct UV (absorbance) detection, or intrinsic fluorescence detection exploiting UV excitation, is practically impossible for most polymers. Instead, bioanalytical processes need to be monitored on the basis of fluorophore tagging of the amino acid residues so that both fluorescence excitation and emission are in the visible range. Even then, attention should be paid on the choice of the fluorophore wavelengths so that detection sensitivity is not restricted by the autofluorescence originating from the chip material.<sup>5,23</sup> Typically, it is the additives that give rise to autofluorescence, with the PDMS and COC being rare exceptions. Thus, the ability to perform efficient optical detection even at near-UV range, makes Ormocomp an ideal material for microfluidics.

## EXPERIMENTAL SECTION

**Materials and Reagents.** Ammonium hydrogen carbonate, monobasic sodium phosphate, disodium phosphate, and  $\beta$ -nicotinamide adenine dinucleotide 2'-phosphate reduced tetrasodium salt (NADPH) were from Sigma-Aldrich (Steinheim, Germany). Boric acid was from Riedel-de Haën (Seelze, Germany), and sodium hydroxide was from Eka Nobel (Bohus, Sweden). Sodium hydrogen carbonate and magnesium chloride were from Merck

(7) Pallandre, A.; de Lambert, B.; Attia, R.; Jonas, A. M.; Viowy, J. L. *Electrophoresis* **2006**, *27*, 584–610.

(8) Makamba, H.; Kim, J. H.; Lim, K.; Park, N.; Hahn, J. H. *Electrophoresis* **2003**, *24*, 3607–3619.

(9) Roman, G. T.; Hlaus, T.; Bass, K. J.; Seelhammer, T. G.; Culbertson, C. T. *Anal. Chem.* **2005**, *77*, 1414–1422.

(10) Kato, M.; Gyoten, Y.; Sakai-Kato, K.; Nakajima, T.; Toyo'oka, T. *Electrophoresis* **2005**, *26*, 3682–3688.

(11) Wang, A. J.; Xu, J. J.; Chen, H. Y. *Anal. Chim. Acta* **2006**, *569*, 188–194.

(12) Xiao, D.; Le, T. V.; Wirth, M. J. *Anal. Chem.* **2004**, *76*, 2055–2061.

(13) <http://www.ormocer.de/EN/>.

(14) Haas, K. H. *Adv. Eng. Mater.* **2000**, *2*, 571–582.

(15) Houbertz, R.; Domann, G.; Cronauer, C.; Schmitt, A.; Martin, H.; Park, J. U.; Frohlich, L.; Buestrich, R.; Popall, M.; Streppel, U.; Dannberg, P.; Wachter, C.; Brauer, A. *Thin Solid Films* **2003**, *442*, 194–200.

(16) Haas, K. H.; Amberg-Schwab, S.; Rose, K. *Thin Solid Films* **1999**, *351*, 198–203.

(17) Schmidt, H. J. *Non-Cryst. Solids* **1985**, *73*, 681–691.

(18) Doraiswamy, A.; Jin, C.; Narayan, R. J.; Mageswaran, P.; Mente, P.; Modi, R.; Auyeung, R.; Chrisey, D. B.; Ovsianikov, A.; Chichkov, B. *Acta Biomater.* **2006**, *2*, 267–275.

(19) Dinca, V.; Ranella, A.; Popescu, A.; Dinescu, M.; Farsari, M.; Fotakis, C. *Appl. Surf. Sci.* **2007**, *254*, 1164–1168.

(20) Aura, S.; Jokinen, V.; Sainiemi, L.; Baumann, M.; Franssila, S. J. *Nanosci. Nanotechnol.* **2009**, *9*, 6710–6715.

(21) Jokinen, V.; Aura, S.; Luosujarvi, L.; Sainiemi, L.; Kotiaho, T.; Franssila, S.; Baumann, M. J. *Am. Soc. Mass Spectrom.* **2009**, *20*, 1723–1730.

(22) Aura, S.; Sikanen, T.; Kotiaho, T.; Franssila, S. *Sens. Actuators, B* **2008**, *132*, 397–403.

(23) Piruska, A.; Nikcevic, I.; Lee, S. H.; Ahn, C.; Heineman, W. R.; Limbach, P. A.; Seliskar, C. J. *Lab Chip* **2005**, *5*, 1348–1354.

(Darmstadt, Germany), and trifluoroacetic acid (TFA) was from Fluka (Buchs, Switzerland). Acetone was from VWR International (Stockholm, Sweden); methanol was from J.T. Baker (Deventer, Holland), and acetonitrile and isopropanol were from Rathburn (Walkerburn, Scotland). All buffer components and solvents were of analytical or HPLC grade. All amino acids, angiotensin I ( $\geq 99.1\%$ ), angiotensin II ( $\geq 96.2\%$ ), substance P (fragment 6–11,  $>97\%$ ), fluorescein isothiocyanate (FITC, isomer I,  $>98.5\%$ ), FITC-labeled BSA (analytical grade), coumarin ( $\geq 99\%$ ), umbelliferone (99%), and scopoletin (99%) were purchased from Sigma-Aldrich. Human liver microsomes (pool of 20 donors) were from BD Biosciences (Erembodegem, Belgium).

**Sample Preparation.** Stock solutions of the L-amino acids (20 mM), peptides (10 mg/mL), BSA (5 mg/mL),  $\beta$ -lactoglobuline (5 mg/mL), and FITC-BSA (15 mg/mL) were prepared in deionized Milli-Q water (Millipore, Bedford, MA) and diluted accordingly with the specified buffer. Umbelliferone and scopoletin were first dissolved in methanol–water (1:1) solution and then diluted with the buffer. Before analysis, all L-amino acids and peptides were individually labeled overnight (16 h) at  $+37^\circ\text{C}$  with a 2-fold molar excess of freshly prepared FITC solution in 50 mM sodium hydrogen carbonate (pH 9.0)–acetone 80:20 (v/v). Before use, all stock solutions and buffer solutions were filtered ( $0.2\ \mu\text{m}$ ) and degassed by sonication for 10 min.

**Enzyme Incubation.** Kinetic parameters of cytochrome P450 (CYP) 2A6 isoenzyme mediated coumarin 7-hydroxylation to umbelliferone were determined by incubating coumarin with human liver microsomes (HLM) under in-house optimized conditions. In brief, coumarin was incubated at  $+37^\circ\text{C}$  in 50 mM sodium phosphate (pH 7.4) buffer including 5 mM magnesium chloride, 0.3 mg/mL human liver microsomes, and with 1 mM NADPH as the cosubstrate. The incubations were performed in duplicate at six different coumarin concentrations in a volume of  $100\ \mu\text{L}$ . After 30 min, the reactions were stopped by the addition of  $100\ \mu\text{L}$  of ice-cold acetonitrile, and the proteins were precipitated by centrifugation (5 min at  $16\ 000g$ ). The supernatant was then spiked with the internal standard ( $5\ \mu\text{M}$  scopoletin) and analyzed using the Ormocomp microchips. The obtained activities of coumarin 7-hydroxylation (in pmol/min/mg protein) were fitted to the Michaelis–Menten equation.

**Microchip Fabrication.** All microchips were fabricated from a commercially available ORMOCER material, Ormocomp (Micro Resist Technology GmbH, Darmstadt, Germany), which is a solvent free, UV-curable inorganic–organic hybrid material. Ormocomp can be patterned using standard UV lithography or UV embossing (Figure 1). Here, UV embossing was done using a transparent PDMS stamp. In addition, double-side polished 7740 Pyrex wafers ( $\varnothing 100\ \text{mm}$ ) were used as substrates for all Ormocomp structures. The microchip designs were based on an accustomed geometry of standard capillary electrophoresis chip incorporating a separation channel (55–85 mm in length) with either double-T ( $100\ \mu\text{m}$ ) or simple injection cross. The microchannel width was typically 30 or  $50\ \mu\text{m}$ . The microchannel height was defined by the layer thickness of the second Ormocomp layer (UV-lithography approach) or by the PDMS stamp height in UV embossing, and it was typically on the order of  $20\ \mu\text{m}$ .

**Ormocomp UV Lithography.** The Pyrex wafers were cleaned with standard RCA 1 cleaning ( $\text{NH}_3/\text{H}_2\text{O}_2/\text{H}_2\text{O}$ , 1:1:5) followed

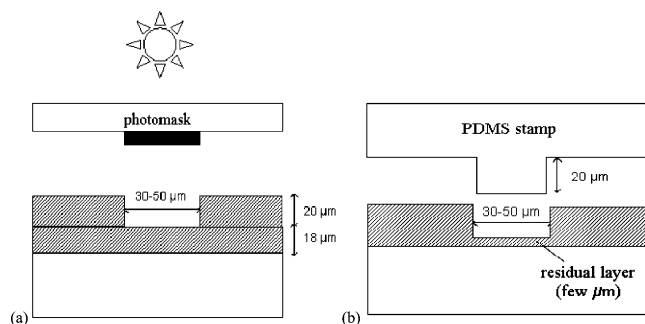


**Figure 1.** (a) Two layer, UV-lithography approach and (b) one layer, UV-embossing approach with a PDMS stamp for Ormocomp micro-channel patterning. In UV embossing (b), the thickness of the bottom Ormocomp layer is defined by the residual layer under the stamp.

by prebaking at  $120^\circ\text{C}$  for at least 1 h to remove moisture from the surface. Next, a layer of Ormocomp was spin-coated (BLE delta 20 BM W8) on the wafer at 6000 rpm for 30 s, which resulted in an Ormocomp thickness of approximately  $18\ \mu\text{m}$ . The wafer was then prebaked on the hot plate at  $+80^\circ\text{C}$  for 2 min after which blank UV exposure (30 s) of the first Ormocomp layer was done with MA 6 mask aligner (SÜSS MicroTec Lithography GmbH, Garching, Germany) at a wavelength of 365 nm ( $30\ \text{mW}/\text{cm}^2$ ). The first layer was then postbaked on the hot plate at  $+80^\circ\text{C}$  for 5 min, and a second layer of Ormocomp was spin-coated on top of the first one at 4000 rpm for 30 s resulting in a thickness of approximately  $21\ \mu\text{m}$ . Since Ormocomp is liquid-like material before exposure, the second Ormocomp layer was UV exposed (5 s) through a photomask in proximity mode. Prebake and postexposure bake were done in a manner similar to those of the first layer. Development of the UV-patterned Ormocomp structures was done with a mixture (1:1) of methylisobutylketone and isopropyl alcohol (i.e., Ormodev from Microresist Technology GmbH) for 3 min followed by a rinse with isopropanol.

**Master Fabrication for UV Embossing.** The master for the fabrication of the PDMS stamp was made from SU-8 50 negative photoresist (Microchem Corporation, Newton, MA). Single-side polished silicon wafers with  $\langle 100 \rangle$  orientation ( $\varnothing 100\ \text{mm}$ ) were used as substrates for the SU-8 patterns. Prior to processing, silicon wafers were cleaned with standard RCA 1 cleaning ( $\text{NH}_3/\text{H}_2\text{O}_2/\text{H}_2\text{O}$ , 1:1:5) followed by prebaking at  $120^\circ\text{C}$  for at least 1 h in order to remove moisture on the surface. Next, SU-8 was spin-coated on the silicon wafer at 500 and 9000 rpm for 10 and 30 s, respectively. The resulting thickness of the SU-8 layer was typically  $20\ \mu\text{m}$ . The wafer was then soft-baked on a hot plate at  $+65^\circ\text{C}$  for 5 min and then at  $+95^\circ\text{C}$  for 8 min after which it was let to cool below  $+50^\circ\text{C}$  before UV exposure. The exposure (15 s) was done through a photomask on a MA 6 mask aligner followed by a postexposure bake on the hot plate at  $+95^\circ\text{C}$  for 8 min and slow cooling to room temperature. The exposed SU-8 patterns were developed in propylene glycol methyl ether acetate (PGMEA) solution for 10 min, rinsed with isopropanol, and dried with nitrogen gas. Last, in order to facilitate PDMS stamp detachment, Teflon-like fluoropolymer was deposited on the wafer in a RIE reactor (Plasmalab 80+, Oxford instruments plasma technology, UK) by applying 100 sccm  $\text{CHF}_3$  source gas flow, 50 W RF-power, and 250 mTorr pressure for 5 min.



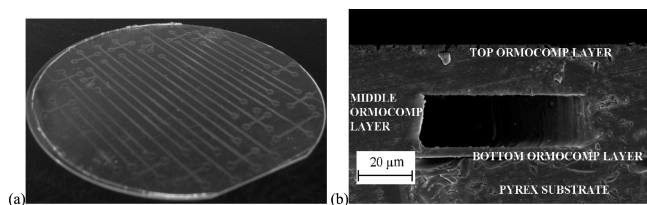


**Figure 2.** (a) A photograph of a full-wafer (diameter 100 mm) array of enclosed Ormocomp separation microchips. (b) A scanning electron micrograph of the cross-section of an Ormocomp separation channel (on Pyrex substrate) demonstrating the good bonding quality between the different Ormocomp layers.

**Embossing Stamp Fabrication.** PDMS stamp was fabricated from Sylgard 184 silicone elastomer (Dow Corning, Midland, MI) by mixing the base elastomer and the curing agent in a ratio of 10:1 (w/w) and degassing the mixture in vacuum before being poured on top of the SU-8 master. The PDMS stamp was cured at 60 °C for 12 h and then peeled off the master.

**Ormocomp UV Embossing.** The Pyrex wafers were pretreated in a manner similar to that in the context of UV lithography. Ormocomp was then spin-coated on the wafer at 500 and 2000 rpm for 10 and 30 s, respectively. The resulting thickness of the Ormocomp layer was typically 70 μm. Embossing was done with the PDMS stamp on the hot plate at +80 °C. Excess air bubbles between the stamp and the Ormocomp layer were removed manually with tweezers after which the exposure (60 s) was done through the stamp. The exposure time as such was not critical since the feature size was defined by the stamp. After exposure, the wafer was transferred onto the hot plate at 80 °C for a postexposure bake during which the stamp was easily peeled off.

**Bonding of Ormocomp Microchannels.** Enclosed Ormocomp microchannels, both lithographically defined and UV embossed, were obtained by exploiting Ormocomp-to-Ormocomp adhesive bonding (Figure 2). Such bonding is facilitated by a thin, uncured Ormocomp film which remains on top of cured Ormocomp layers when exposure is done in the presence of oxygen. Here, an Ormocomp bonding layer was spin-coated on top of a standard overhead transparency cleaned with acetone and attached onto a carrier wafer with double-sided tape. Spin-coating was done at 500 and 4000 rpm for 10 and 30 s, respectively, after which the Ormocomp layer was soft-baked at +80 °C for 2 min and flood-exposed for 20 s. Next, the transparency was detached from the carrier wafer and assembled on top of the previously patterned Ormocomp wafer incorporating the microchannels. The two Ormocomp layers were then manually pressed together with tweezers, and a flood exposure of 30 s was done through the transparency to finalize adhesion. Last, the transparency was detached from the Ormocomp layers. The resulting thickness of the top (bonding) Ormocomp layer was typically 18 μm.

**Instrumentation.** The performance of the Ormocomp microchips was characterized utilizing microchip capillary (zone) electrophoresis (MCE), electroosmotic flow (EOF) measurements, and fluorescence microscopy. Where applicable, the performance of the Ormocomp microchips was examined against commercial low fluorescence Schott Borofloat glass microchips (model MC-BF4-TT100, Micralyne, Edmonton, Canada).

**Microchip Capillary Electrophoresis.** A computer-controlled (Labview) high voltage power supply (Microfluidic Tool Kit, Micralyne, Edmonton, Canada) was used for application of the

separation voltages and to record current readings during experiments. Before use, all microchannels were sequentially rinsed with 0.5 M sodium hydroxide, deionized water, and the specified separation buffer for 2, 2, and 5 min, respectively, by applying vacuum to a microchannel inlet. After rinsing, the microchannels were filled with fresh buffer solution and quantities of 20, 20, and 10 μL of the buffer were applied to the buffer inlet, buffer waste, and sample waste reservoirs, respectively. Last, an aliquot of 5–10 μL of the sample solution was applied to the sample inlet followed by immediate application of the injection voltages. Sample introduction was performed in pinched injection mode at 1000 V/cm for 15–20 s. The separation conditions were optimized with respect to the separation buffer composition and the electric field strength. In order to prevent sample leakage, small push-back voltages were typically applied to the sample inlet and sample waste during separation.

**EOF Determination.** The EOF velocities were determined on the basis of the current monitoring method.<sup>24</sup> All measurements were performed with the same instrumentation as in the MCE experiments except that a 500 kΩ resistor was coupled in series with the microchannel and the current changes over time, calculated on the basis of the observed voltage drop across the resistor, were monitored using the PicoScope 2203 AD converter. Typically, a 5% decrease in the electrolyte concentration was utilized in order to induce current drop in the circuit. The applied electric field strength during measurements was between 300 and 700 V/cm.

**Fluorescence Microscopy.** Fluorescence detection of the FITC-conjugates was accomplished with a Leica DMIL inverted epifluorescence microscope (Leica Nilomark, Espoo, Finland) equipped with an N PLAN 10 × /0.25 objective and a 75 W xenon arc lamp with integrated lamp housing (Cairn Research, Faversham, UK). The fluorescence excitation (450–490 nm) and emission (515–600 nm) ranges were defined by appropriate filters.

Native fluorescence detection at 355 nm (excitation wavelength) was accomplished with a Zeiss Axioscope A1 upright epifluorescence microscope (Carl Zeiss Oy, Espoo, Finland) equipped with a Plan-Neofluar 40 × /0.4 Corr objective and a PowerChip-PNV diode-pumped UV355 nm laser (15 μJ at 1 kHz) with custom-made laser housing (Cheos Oy, Espoo, Finland). The fluorescence emission range (400–700 nm) was defined by appropriate emission filters.

Both microscopes were equipped with a similar Hamamatsu R5929 photomultiplier tube with integrated housing and a signal amplifier module (Cairn Research). Fluorescence emission was collected perpendicular to the microchip by defining a detection slit of 50 μm × (70–200) μm on top of the microchannel at a predefined detection distance. A PicoScope 2203 AD converter and PicoLog software (Pico Technology, St. Neots, UK) were used for recording the signal acquired from the photomultiplier tube.

## RESULTS AND DISCUSSION

In this study, for the first time, fully enclosed all-Ormocomp microchannels were fabricated by either UV lithography or UV embossing followed by adhesive bonding of the roof layer also made from Ormocomp. The enclosed Ormocomp channels were utilized in MCE separation of fluorescent labeled proteins, pep-

(24) Huang, X. H.; Gordon, M. J.; Zare, R. N. *Anal. Chem.* **1988**, *60*, 1837–1838.

tides, and amino acids. The surface chemistry and biocompatibility of native (untreated) Ormocomp microchannels, fabricated by both lithographic and embossing techniques, were examined and compared. Finally, the optical properties of Ormocomp microchips were assessed against those of commercial, low-fluorescent Borofloat glass microchips by determining the sensitivity of label-free (intrinsic) fluorescence detection at near-UV (ex 355 nm) range.

**Surface Charge and Electroosmotic Flow.** The surface charge was first determined for both lithographically defined and UV-embossed Ormocomp microchannels by following the EOF velocity according to the current monitoring method.<sup>24</sup> The electroosmotic (EO) mobilities were measured under comparable conditions for 18 mM sodium borate buffer (pH 10.0) and were  $(3.3 \pm 0.3) \times 10^{-8} \text{ m}^2\text{V}^{-1}\text{s}^{-1}$  and  $(5.3 \pm 0.1) \times 10^{-8} \text{ m}^2\text{V}^{-1}\text{s}^{-1}$  for lithographically defined and UV-embossed microchannels ( $n = 6$  runs), respectively. The corresponding zeta potential values were calculated as per the Smoluchowski equation and were  $-41.8 \pm 3.2$  and  $-65.9 \pm 1.5$  mV, respectively. The observed differences in the surface charge were likely to result from the different fabrication conditions between different methods and also between different batches of microchips fabricated by the same method. Previous studies support the fact that a relatively large deviation (typically 15–30% RSD) can be attributed to the batch-to-batch variation between both polymer and glass microchannels fabricated by exactly the same method.<sup>25–27</sup> Others have also shown that, besides material itself, EOF in polymer microchannels may also depend on the fabrication method. These kind of effects have been observed for instance between hot embossed and laser ablated PMMA<sup>28</sup> or COC<sup>29,30</sup> microchannels. In this study, the measured batch-to-batch ( $n = 3$ ) deviations were 19.0% and 12.9% (RSD) for lithographically defined and UV-embossed microchannels, respectively, and thus, in good accordance with the previous literature. In all cases, however, substantial EOF with relatively low run-to-run repeatability (typically 4–7%) was observed, indicating high surface charge density and stable surface charge equilibrium on both lithographically defined and UV-embossed Ormocomp surfaces.

**Surface Interactions and Biofouling Resistance.** The biocompatibility of Ormocomp was examined by screening the surface interactions between Ormocomp and selected model compounds, i.e., bovine serum albumin (BSA) and a set of L-amino acids possessing different properties. The separation media (18 mM sodium borate (pH 10.0) buffer) was chosen on the basis of two arguments. Namely, the relatively high ionic strength and high pH (above the pI values of the model compounds) enabled elimination of electrostatic interactions on the microchannel wall and, thus, examination of interactions of purely hydrophobic–

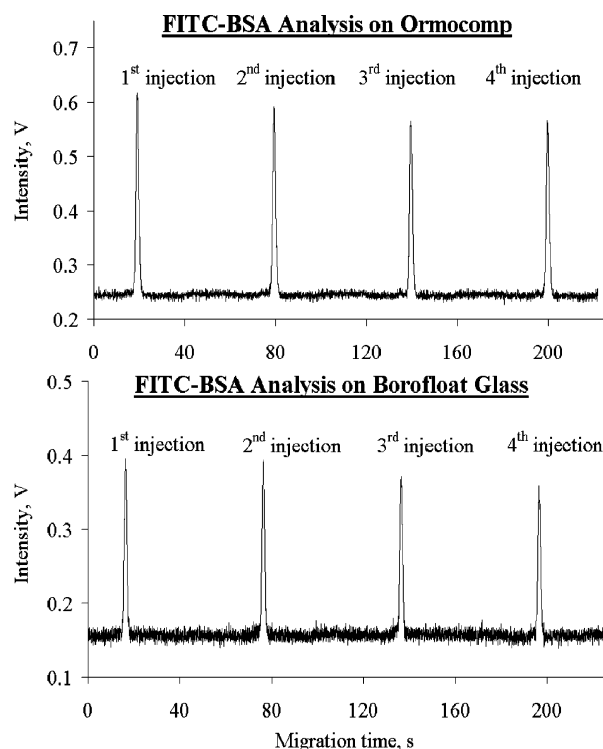


**Figure 3.** MCE analyses of FITC-derivatized BSA (2.5 mg/mL) in 18 mM sodium borate (pH 10.0) using a lithographically defined Ormocomp microchip (upper panel) or Borofloat glass microchip (lower panel). The injections were performed in pinched injection mode at  $1200 \text{ Vcm}^{-1}$  for 20 s, and the separations were performed at  $620 \text{ Vcm}^{-1}$ . The distance of detection was 4.0 cm (both microchips).

hydrophilic origin. In addition, high pH also assured maximum fluorescence intensity from the FITC-derivatized biomolecules.<sup>31</sup>

BSA is a high molecular weight (66 kDa) protein which is known to easily adhere to most plastic surfaces. Here, a commercial fluorescein conjugate, FITC–BSA, was utilized to study the biofouling resistance of Ormocomp by means of MCE and fluorescence detection (ex 488 nm) of the conjugate. Repeated injections of FITC–BSA were done under conditions described in Figure 3 using both lithographically defined and UV-embossed Ormocomp microchips. Borofloat glass microchips, known to be less vulnerable to biofouling, were used for comparison. This allowed us to compare the effects of nonspecific adsorption of FITC–BSA on the analytical parameters between materials. As a result, Ormocomp was found to effectively resist protein adsorption without any surface modification after microfabrication or without any surface active ingredients applied prior to analysis. The repeatabilities of the FITC–BSA migration time from run to run were 0.9% and 1.9% (RSD,  $n = 4$ ) for untreated lithographically defined and UV-embossed Ormocomp microchannels, respectively. These values were well below the run-to-run variation induced by EOF (i.e., 4–7% RSD in Ormocomp microchannels) and were also consistent with the FITC–BSA migration time repeatability measured for Borofloat glass microchips (1.1% RSD,  $n = 4$ ). The number of theoretical plates was as high as  $(1.8 \pm 0.2) \times 10^4 \text{ m}^{-1}$  for FITC–BSA analysis in Ormocomp microchannels, against a plate number of  $(1.0 \pm 0.2) \times 10^4 \text{ m}^{-1}$  for

(25) Locascio, L. E.; Perso, C. E.; Lee, C. S. *J. Chromatogr., A* **1999**, *857*, 275–284.

(26) Sikanen, T.; Tuomikoski, S.; Ketola, R. A.; Kostianen, R.; Franssila, S.; Kotiaho, T. *Lab Chip* **2005**, *5*, 888–896.

(27) Sikanen, T.; Heikkilä, L.; Tuomikoski, S.; Ketola, R. A.; Kostianen, R.; Franssila, S.; Kotiaho, T. *Anal. Chem.* **2007**, *79*, 6255–6263.

(28) Johnson, T. J.; Waddell, E. A.; Kramer, G. W.; Locascio, L. E. *Appl. Surf. Sci.* **2001**, *181*, 149–159.

(29) Gaudioso, J.; Craighead, H. G. *J. Chromatogr., A* **2002**, *971*, 249–253.

(30) Mela, P.; van den Berg, A.; Fintschenko, Y.; Cummings, E. B.; Simmons, B. A.; Kirby, B. J. *Electrophoresis* **2005**, *26*, 1792–1799.

(31) Lanz, E.; Gregor, M.; Slavik, J.; Kotyk, A. *J. Fluoresc.* **1997**, *7*, 317–319.

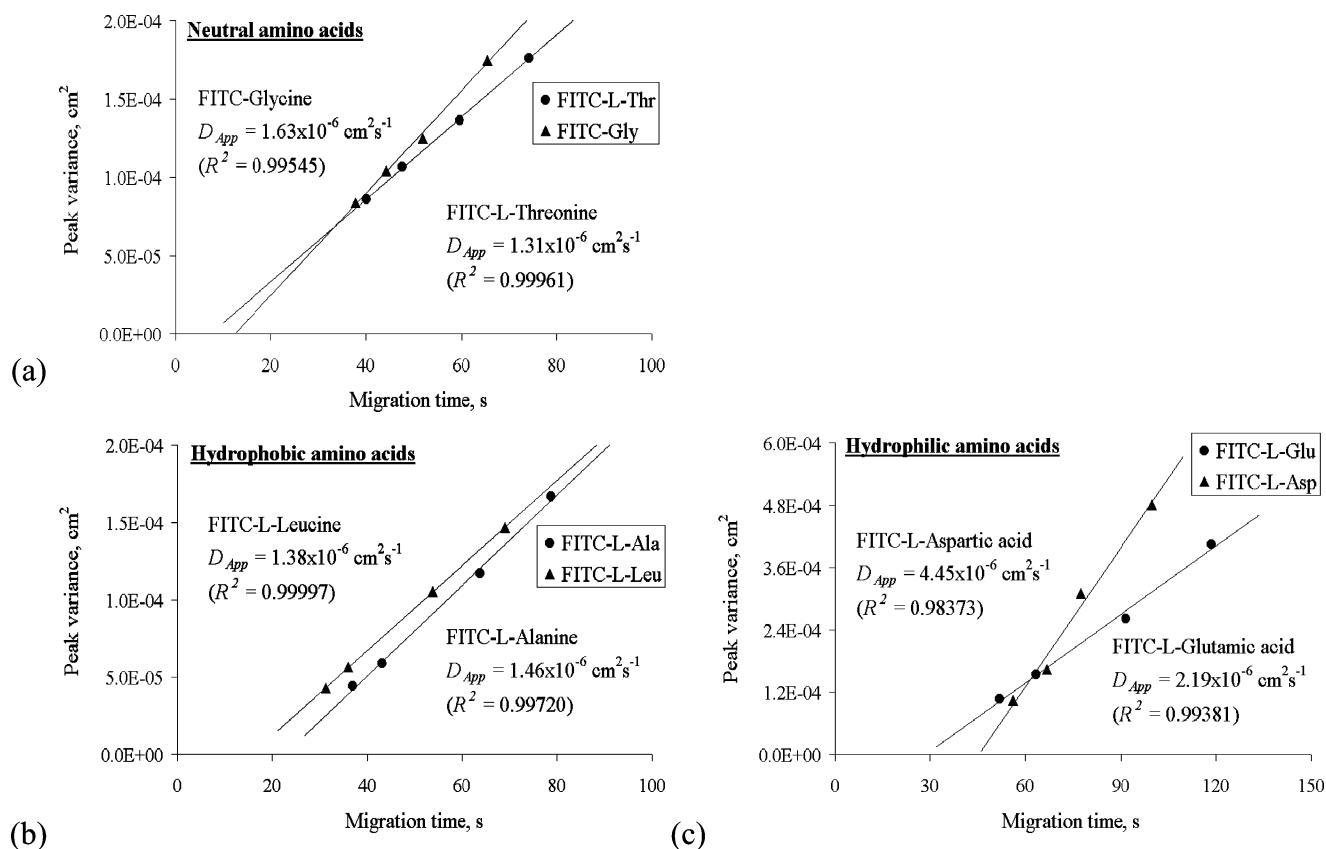


**Figure 4.** Apparent diffusion coefficients of (a) neutral, (b) hydrophobic, and (c) hydrophilic FITC-L-amino acids (50  $\mu\text{M}$ ) determined by plotting the spatial peak variance as a function of migration time at different electric field strengths. The analyses were done in 18 mM sodium borate (pH 10.0) using lithographically defined Ormocomp microchips. The injections were performed in pinched injection mode at 1200  $\text{V cm}^{-1}$  for 20 s. The distance of detection was constantly at 4.0 cm, and the electric field strengths were 360–450–630–720  $\text{V cm}^{-1}$  (Ala, Leu, and Glu), 360–450–540–630  $\text{V cm}^{-1}$  (Thr), or 450–540–630–720  $\text{V cm}^{-1}$  (Gly and Asp).

Borofloat glass microchannels. The peak profile (width, asymmetry) was also perfectly comparable between runs made by Ormocomp and Borofloat glass chips (Figure 3), suggesting negligible interactions between the protein and the Ormocomp surface.

Next, selected L-amino acids were labeled in-house with FITC and analyzed by MCE and fluorescence detection (ex 488 nm) in a similar manner than FITC-BSA. Altogether six amino acids were included, two of which were classified as hydrophilic (i.e., aspartic acid (Asp) and glutamic acid (Glu)), two as neutral (i.e., glycine (Gly) and threonine (Thr)), and two as hydrophobic (i.e., leucine (Leu) and alanine (Ala)).<sup>32</sup> As a result, all amino acids, regardless of hydrophobicity or charge state (pI), provided symmetric peaks with plate numbers of  $(3.5\text{--}5.3) \times 10^5 \text{ m}^{-1}$ .

In order to confirm the absence of nonspecific interactions, the apparent diffusion coefficients ( $D_{App}$ ) were determined for each amino acid selected through a series of runs performed at a detection distance of 4.0 cm but at different electric field strengths (according to Yao and Li<sup>33</sup>). By plotting spatial peak variance ( $\sigma^2$ ) against migration time ( $t$ ), a linear regression results if band broadening is due to random processes only. The slope of the regression line is twice the value of the apparent diffusion coefficient ( $\sigma^2 = 2Dt$ ), and the better the correlation coefficient ( $R^2$ ), the less are the nonspecific interac-

tions. As can be seen from Figure 4, the spatial peak variances of all amino acids followed linear regressions with correlation coefficients between 0.98373 and 0.99997, confirming that band broadening in Ormocomp microchannels was mainly diffusion limited. Although the relatively large fluorescein label (FITC) is likely to dominate the diffusion behavior, subtle differences were observed between amino acids. For instance, the apparent diffusion coefficients of hydrophobic and neutral amino acids were found to decrease with increasing molecular volume (taking into account molecular weight and hydrophobicity):  $D_{App}(\text{Gly}) > D_{App}(\text{Ala}) > D_{App}(\text{Leu}) > D_{App}(\text{Thr})$ . Such behavior is similar to that earlier observed in studies on the diffusion coefficients of native (unlabeled) amino acids in aqueous solutions.<sup>34</sup> However, according to Ma and co-workers,<sup>34</sup> the diffusion coefficient also decreases with increasing polarity, which was not the case in our experiments. Instead, the apparent diffusion coefficients of hydrophilic amino acids were somewhat higher ( $2.19\text{--}4.45 \times 10^{-6} \text{ cm}^2 \text{s}^{-1}$ ) than those of hydrophobic or neutral amino acids ( $1.31\text{--}1.63 \times 10^{-6} \text{ cm}^2 \text{s}^{-1}$ ), indicating that minor band broadening may occur because of hydrophilic interactions (e.g., hydrogen bonding) on Ormocomp surfaces. Nevertheless, the obtained diffusion coefficients were generally in good agreement with those earlier reported for both FITC-labeled

(32) Kyte, J.; Doolittle, R. F. *J. Mol. Biol.* **1982**, *157*, 105–132.

(33) Yao, Y. J.; Li, S. F. Y. *J. Chromatogr. Sci.* **1994**, *32*, 117–120.

(34) Ma, Y.; Zhu, C.; Ma, P.; Yu, K. T. *J. Chem. Eng. Data* **2005**, *50*, 1192–1196.



amino acids  $((3.0\text{--}3.9) \times 10^{-6} \text{ cm}^2\text{s}^{-135})$  and fluorescein itself  $((3.3\text{--}4.25) \times 10^{-6} \text{ cm}^2\text{s}^{-13,36})$ , although direct comparison is not possible because of different experimental conditions. Altogether, the results confirmed that both lithographically defined and UV-embossed Ormocomp surfaces are natively resistant to biofouling. This is also in line with the previous results on the good biocompatibility of Ormocomp regarding cell viability and cell growth on Ormocomp surfaces.<sup>18</sup>

**Intrinsic Laser-Induced Fluorescence Detection.** The sensitivity of optical detection techniques does not directly benefit from miniaturization. Nevertheless, fluorescence detection, laser-induced fluorescence (LIF) in particular, remains as the most sensitive technique available for microfluidic applications to such a degree that single-molecule detection has been accomplished.<sup>37,38</sup> However, only a few compounds are inherently fluorescent at visible range, and they must be derivatized to allow detection through polymer-based substrates. On the other hand, most compounds, such as many drugs and proteins, exhibit intensive fluorescence at UV range, which is by default not accessible through polymer substrates. This is why label-free detection of underivatized compounds, so-called native fluorescence, is extremely rare among microfluidic applications.

In this study, a diode-pumped near-UV (355 nm, 15 mW) laser was used for LIF detection of inherently fluorescent coumarin dyes, umbelliferone and scopoletin, through Ormocomp microstructures. The MCE separation conditions were first optimized with respect to buffer composition and electric field strength, and a linear correlation of  $R^2=0.9939$  was established for umbelliferone over a concentration range of 500 nM to 2.5  $\mu\text{M}$ , using scopoletin (5  $\mu\text{M}$ ) as an internal standard. The limits of detection (LOD) and quantitation (LOQ) of umbelliferone were 207 and 626 nM, respectively, as per ICH validation guidelines (based on the standard deviation of the response and the slope of a calibration curve). The repeatabilities for the relative peak area (RSD,  $n = 6$ ) were also determined close to the lower (750 nM) and upper (2.5  $\mu\text{M}$ ) level of quantitation and were 3.0 and 5.3%, respectively, suggesting good analytical reproducibility from run to run. The MCE separation of 5  $\mu\text{M}$  scopoletin (internal standard) and 250 nM umbelliferone (close to its LOD) is presented in Figure 5a. For comparison, the corresponding, in-house determined LOD and LOQ values through low-fluorescent Borofloat glass were nearly the same, namely 163 nM (LOD) and 494 nM (LOQ), suggesting equally low background interference from Ormocomp or Borofloat glass. In addition, the detection limits obtained were equal to those previously reported for selected pharmaceuticals (81–475 nM) by label-free UV–LIF detection through quartz substrates.<sup>39</sup> Thus far, deep UV (266 nm) fluorescence detection has only been accomplished using PDMS- or quartz-based microchips.<sup>40,41</sup> Less UV-transparent glass materials, such as Pyrex or Borofloat, have also been used when

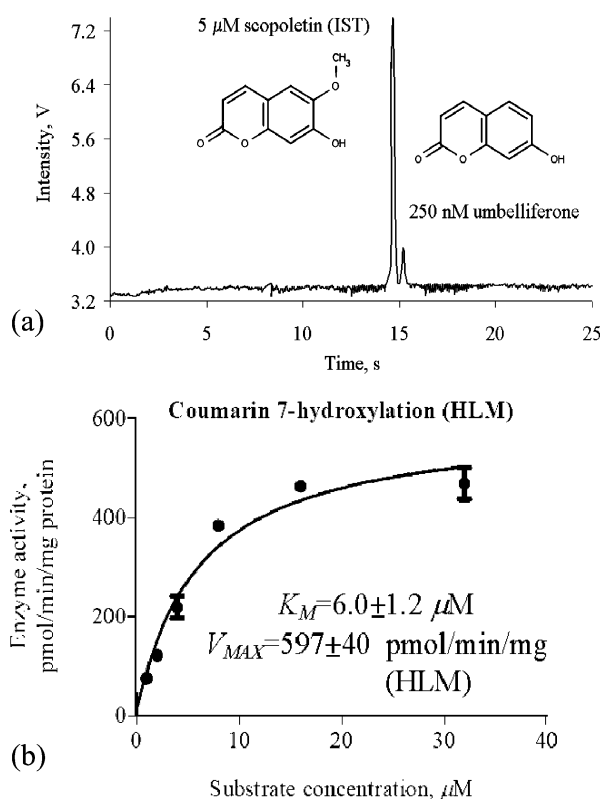


**Figure 5.** (a) MCE separation of scopoletin (5  $\mu\text{M}$ ) and umbelliferone (250 nM) in 18 mM sodium borate (pH 10.0) at 440  $\text{Vcm}^{-1}$ . The injection was performed in pinched injection mode at 1000  $\text{Vcm}^{-1}$  for 20 s. The distance of detection was 3.5 cm. (b) Michaelis–Menten fit for coumarin 7-hydroxylation in human liver microsomes (HLM) as determined using the Ormocomp chip. The separation conditions were as in (a).

excitation wavelengths have been at near-UV (300–385 nm)<sup>42</sup> or visible (488 nm) range<sup>43</sup> or when two-photon excited fluorescence has been utilized in order to overcome background interference.<sup>44</sup> At best, detection limits between 81 and 475 nM have been reported for small drug compounds and proteins by deep-UV (266 nm, 120 mW) excitation.<sup>39</sup> A low micromolar detection limit was also reported for Titan Yellow at near-UV (300–385 nm) excitation, though a mercury lamp was used for excitation instead of a high-power laser.<sup>42</sup>

Next, the Ormocomp chips were exploited in the analysis of in vitro metabolism samples in order to examine the applicability of intrinsic LIF detection through Ormocomp to real analytical tasks. Kinetic parameters of cytochrome P450 (CYP) 2A6 isoenzyme mediated coumarin 7-hydroxylation to umbelliferone were determined using off-chip incubated samples spiked with an internal standard (5  $\mu\text{M}$  scopoletin) and analyzed under separation conditions described in Figure 5a. The obtained Michaelis–Menten parameters for coumarin 7-hydroxylation were  $K_M = 6.0 \pm 1.2 \mu\text{M}$  and  $V_{\text{MAX}} = 597 \pm 40 \text{ pmol/min/mg protein}$  (Figure 5b). These values were in accordance with the previously reported

(35) Effenhauser, C. S.; Manz, A.; Widmer, H. M. *Anal. Chem.* **1993**, *65*, 2637–2642.

(36) Culbertson, C. T.; Jacobson, S. C.; Ramsey, J. M. *Talanta* **2002**, *56*, 365–373.

(37) Fister, J. C.; Jacobson, S. C.; Davis, L. M.; Ramsey, J. M. *Anal. Chem.* **1998**, *70*, 431–437.

(38) Shelby, J. P.; Chiu, D. T. *Anal. Chem.* **2003**, *75*, 1387–1392.

(39) Schulze, P.; Ludwig, M.; Belder, D. *Electrophoresis* **2008**, *29*, 4894–4899.

(40) Schulze, P.; Ludwig, M.; Kohler, F.; Belder, D. *Anal. Chem.* **2005**, *77*, 1325–1329.

(41) Ros, A.; Hellmich, W.; Leffhalm, K.; Sischka, A.; Anselmetti, D. *Mol. Cell. Proteomics* **2005**, *4*, S336–S336.

(42) Yan, Q.; Chen, R. S.; Cheng, J. *Anal. Chim. Acta* **2006**, *555*, 246–249.

(43) Liu, B. F.; Hisamoto, H.; Terabe, S. *J. Chromatogr., A* **2003**, *1021*, 201–207.

(44) Schulze, P.; Schuttpelz, M.; Sauer, M.; Belder, D. *Lab Chip* **2007**, *7*, 1841–1844.

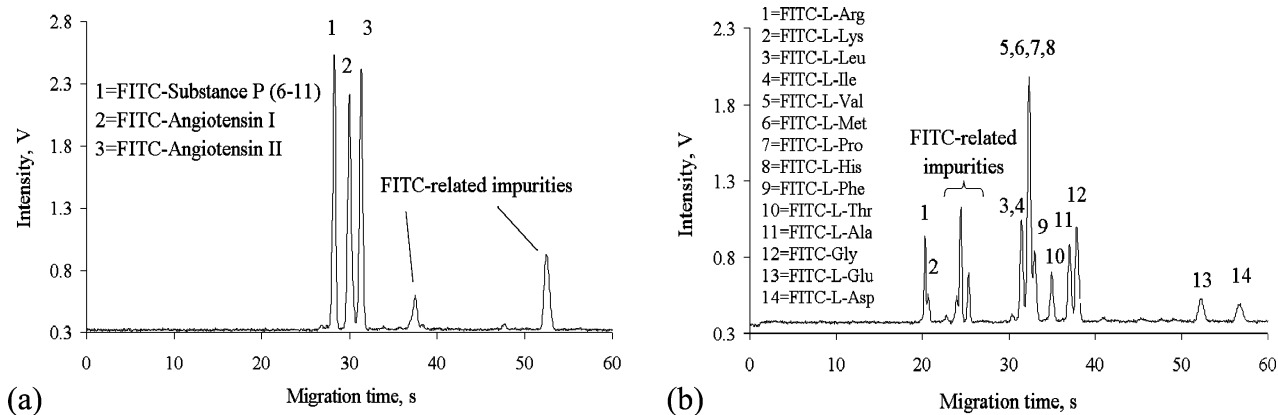


**Figure 6.** (a) MCE separation of FITC-labeled substance P (6-11), angiotensin I, and angiotensin II (all 200  $\mu\text{M}$ ) in 18 mM sodium borate (pH 10.0) at 300  $\text{V cm}^{-1}$ . The injection was performed in pinched injection mode at 1200  $\text{V cm}^{-1}$  for 15 s. The distance of detection was 4.0 cm. (b) MCE separation of FITC-labeled L-amino acids (all 50  $\mu\text{M}$ ) in 36 mM sodium borate (pH 10.0) at 720  $\text{V cm}^{-1}$ . The injection was performed in pinched injection mode at 1200  $\text{V cm}^{-1}$  for 20 s. The distance of detection was 4.5 cm.

parameters of coumarin 7-hydroxylation in human liver microsomes, i.e.,  $K_M$  values between 0.2 and 2.3  $\mu\text{M}$ .<sup>45–47</sup>

Clearly, the results suggest that Ormocomp structures can be utilized as more economic alternatives to highly expensive and rare quartz microchips in optical detection even at UV range. Although deep-UV range (<300 nm) can hardly be reached, LIF detection at near-UV range enables numerous possibilities for label-free analysis. Often, the deep-UV range is also inaccessible to standard microscope optics that are commonly made from borosilicate and show high transparency only at excitation wavelengths above 300 nm (and autofluoresce when excited by deep UV). Nevertheless, near-UV range between 330 and 380 nm forms an absorption zone characteristic for many pharmaceuticals (e.g., hallucinogens, diuretics, nonsteroidal antiinflammatories) and Ormocomp enables their label-free detection by LIF.

**Separation Performance.** Materials properties, both surface and bulk, have their implications on the resulting performance of the separation system in question. Obviously, all nonspecific surface interactions need to be eliminated in order to achieve maximum performance through narrower peak width. In addition, the better the detection sensitivity, the smaller is the risk of contamination since lower concentrations can be used. It is also clear that the stability of the surface charge and EOF greatly affect the analytical reproducibility. According to our results, Ormocomp appears as an ideal chip fabrication material for high-efficiency bioseparations because of its favorable and inert surface chemistry and good optical transparency. The results suggest that analytical performance similar to that of glass-based devices is easily obtained using Ormocomp microchips. As an example, fast (<60 s) and highly efficient separation of FITC-labeled peptides, with plate numbers reaching record-breaking million plates per meter (i.e.,  $(2.6\text{--}3.2) \times 10^4$  plates per separation length of 4.0 cm), was demonstrated using Ormocomp microchannels (Figure 6a). Similar separation efficiency, i.e.,  $(2.5\text{--}3.8) \times 10^4$  plates per separation length of 4.5 cm, was also obtained for FITC-labeled

L-amino acids within 60 s (Figure 6b). The peak widths were on the order of 0.4 s for the peptides and between 0.4 and 0.8 s for the amino acids, and the migration time repeatabilities (RSD,  $n = 4$ ) with and without internal standard were 0.05–0.53% (amino acids) and 1.9–2.2% (peptides), respectively. These values are in general better than those previously reported for microchip-based separations of fluorescent labeled peptides<sup>12,27</sup> or amino acids,<sup>9,10,48</sup> though direct comparison is hardly possible due to differences in the experimental conditions and fluorescent labels.

The results also show that, under extreme conditions, the absolute EOF velocity may have a decisive role in defining the final separation efficiency. In general, EOF velocity attributed to polymer-based microchips is lower than that of glass-based microchips.<sup>5</sup> This allows extension in the separation time and, thus, better resolving power if nonspecific interactions of analytes can be eliminated. In our work, the effect of EOF velocity was found especially crucial on the separation of the coumarin derivatives presented in Figure 5a. Umbelliferone and scopoletin are weakly acidic in nature ( $\text{p}K_a \sim 9.0\text{--}9.5$ ) and differ from one another only by the neutral methoxy group. Despite their very similar electrophoretic mobilities, scopoletin and umbelliferone were resolved ( $R_s = 1.1$ ) within 15 s and had a separation path of 3.5 cm in Ormocomp microchannels. Meanwhile, the same resolution in Borofloat glass microchannels was not possible unless the separation length was extended to 6.0 cm and 5% isopropanol was added to the separation buffer.

## CONCLUSIONS

A new, nonbiofouling material, Ormocomp, was introduced for the fabrication of microfluidic separation chips. Ormocomp was patterned by two independent techniques, i.e., photolithography and UV embossing, resulting in similar biocompatibility and surface properties of the end product. Enclosed microstructures with all inner surfaces of the same material were obtained through adhesive bonding of Ormocomp layers. The physicochemical properties of Ormocomp were characterized by means of microchip capillary electrophoresis (MCE) and fluorescence detection of a variety of biologically active compounds, i.e., amino acids,

(45) Pelkonen, O.; Sotaniemi, E. A.; Ahokas, J. T. *Br. J. Clin. Pharmacol.* **1985**, *19*, 59–66.

(46) Pearce, R.; Greenway, D.; Parkinson, A. *Arch. Biochem. Biophys.* **1992**, *298*, 211–225.

(47) Draper, A. J.; Madan, A.; Parkinson, A. *Arch. Biochem. Biophys.* **1997**, *341*, 47–61.

(48) Culbertson, C. T.; Jacobson, S. C.; Ramsey, J. M. *Anal. Chem.* **2000**, *72*, 5814–5819.



peptides, and intact proteins. It was shown that regarding separation efficiency and detection sensitivity, in particular, Ormocomp holds a record-breaking performance over most other polymers so far introduced to microfluidics. This is because Ormocomp was found to be natively resistant to biofouling and to maintain stable cathodic EOF on the order of  $(3-5) \times 10^{-8} \text{ m}^2\text{V}^{-1}\text{s}^{-1}$  (in 18 mM sodium borate at pH 10). As a result, theoretical separation plates of up to  $10^6$  per meter were easily obtained for fluorescently labeled amino acids and peptides by MCE in Ormocomp microchannels. Good separation efficiency ( $\sim 10^4$  plates per meter) was also obtained in intact protein analysis without any chemical or physical modification of the native Ormocomp surfaces. In addition, Ormocomp enabled highly sensitive intrinsic fluorescence detection even at near-UV range (ex 355 nm) so that detection limits at nanomolar level ( $\sim 200 \text{ nM}$ ) were reached for inherently fluorescent

pharmaceuticals. According to our results, Ormocomp appears as an ideal chip fabrication material for microfluidic bioanalysis, especially when material biocompatibility is of paramount concern.

#### ACKNOWLEDGMENT

The work was financially supported by the Academy of Finland (121882), the Finnish Funding Agency for Technology and Innovation (40380/06), the University of Helsinki Research Funds, and the Graduate School of Electrical and Communication Engineering. Ms. Elisa Moilanen is gratefully acknowledged for her help with the metabolism assays.

Received for review February 13, 2010. Accepted April 6, 2010.

AC1004053